J Mater Sci (2010) 45:2474–2483
DOI 10.1007/s10853-010-4219-8

Supramolecular host–guest systems constructed of pyrrole derivatives and 3D-coordination polymers

Safaa Eldin H. Etaiw · Moustafa Sh. Ibrahim · Dina M. Abd El-Aziz

Received: 5 October 2009 / Accepted: 9 January 2010 / Published online: 27 January 2010

Abstract Pyrrole derivatives have been shown to be completely or partially oxidized within the expandable channels of the 3D-coordination polymers $[(R_3Sn)_3Fe(CN)_6]_n$ and $[(R_3Sn)(R'_3Sn)_2Fe(CN)_6]_n$, R and R′ = Me, *n*-Bu, or Ph, to give novel class of supramolecular host–guest systems. The structures and physical properties of these host–guest systems depend on the reaction time, nature of the host and guest, the space empty within the network of the 3D-coordination polymers. Pyrrole undergoes oxidative polymerization in the channels of the 3D-coordination polymers to form semiconducting diamagnetic supramolecular host–guest systems. Whereas *N*-methylpyrrole and 2,5-dimethylpyrrole are not polymerized under these experimental conditions, but give paramagnetic charge transfer (CT) supramolecular host–guest systems.

Introduction

The term coordination polymer very broadly encompasses any extended structure based on metal ions linked into an infinite chain, sheet, or three-dimensional architecture by bridging ligands, usually containing organic carbon [1]. The self-assembly reactions of the binary adducts of R_3SnCl and hexacynoferrate afford 3D-coordination polymers of the type $[(R_3Sn)_3Fe(CN)_6]_n$, R = alkyl or aryl as was supported by X-ray single crystal studies [2–4]. This type of coordination polymers are example of guest-free cyanide bridged 3D-networks which are composed of distorted octahedral $[Fe(CN)_6]$ building blocks connected by (R_3Sn) bridges through the cyanide N atoms forming three infinite nonlinear chains. These compounds have zeolite-like structures with remarkably wide parallel channels of diameter ca. 8.8–9.5 Å [4–7]. These 3D-coordination polymers have different potential applications as they act as ion exchangers [8], oxidative materials [9–12], zeolite-like catalysis, molecular sieves, 3D-hosts and also as acceptors forming charge transfer complexes (CTC) [4, 13–16]. The host attractive properties arise from the availability of the wide channels for trapping organic and organometallic guest cations G^{n+} into the negatively charged host lattice $[(R_3Sn)_3Fe^{II}(CN)_6^-]_n$ formed by reduction of the isostructural Fe^{III} homologue [14]. One of the main potential applications of the 3D-coordination polymers is the preparation of a new class of semiconducting polymers. In which, these 3D-coordination polymers are insulators at room temperature, but when some heterocyclic compounds have been encapsulated within their channels, semiconducting supramolecular polymers should be obtained [13, 14]. Pyrrole compounds have received considerable attention due to their lower oxidation potential of 0.8 V (SCE) [14]. On the other hand, the anion $[Fe(CN)_6]^{3-}$ is a mild oxidant whose reduction potential is around 0.41 V [3]. This trend is in agreement with the reducing ability of pyrrole compounds toward the 3D-coordination polymers.

In this study, the encapsulation of some pyrrole derivatives acting as guest materials within the channels of the 3D-coordination polymers (host matrix) $[(R_3Sn)_3Fe(CN)_6]_n$ and $[(R_3Sn)(R_3'Sn)_2Fe(CN)_6]_n$, R and R′ = Me, *n*-Bu, or Ph, gives novel semiconducting supramolecular host–guest systems. Also, this study reports the formation of paramagnetic CTCs.

S. E. H. Etaiw (✉) · M. Sh. Ibrahim · D. M. Abd El-Aziz
Department of Chemistry, Faculty of Science, University of Tanta, Tanta, Egypt
e-mail: safaaetaiw@yahoo.com

Experimental

Materials and preparations

All chemicals used in this study were the purest grade and used without further purification. However, pyrrole and its derivatives were doubly distilled in the dark under vacuum before use and stored in a sealed ampoule under nitrogen atmosphere. The 3D-coordination polymers of the type $[(R_3Sn)_3Fe(CN)_6]_n$, where R = *n*-Bu (I) or Ph (II) were prepared by mixing an aqueous solution of $K_3[Fe(CN)_6]$ and a stirred solution of R_3SnCl in (H_2O/acetone), in the molar ratio 1:3.

The novel mixed bridging organotin-connecting units were prepared by mixing two different organotin chlorides R_3SnCl and R'_3SnCl, R and R′ = Me, *n*-Bu, or Ph, with respect to the desired reaction stoichiometry and were added to an aqueous solution of $K_3[Fe(CN)_6]$.

In all cases, gelatinous precipitates were formed immediately after mixing, which were filtered off and repeatedly washed with distilled H_2O and acetone, then finally dried under vacuum at room temperature before use. The purity and identity of the 3D-coordination polymers were checked by elemental analysis, IR, and UV spectroscopy. The supramolecular host–guest systems were prepared by tribochemical reaction of the dry freshly prepared 3D-coordination polymers at room temperature with an excess amount of the neat doubly distilled pyrrole and its derivatives namely; pyrrole, *N*-methylpyrrole, 2,5-dimethylpyrrole. The mixture was kept together with continuous slight grinding for 2 days, whereas the reaction time in the case of *N*-methylpyrrole and 2,5-dimethylpyrrole reached to 7–10 days. The reaction rate was greatly increased by the addition of few drops of water. After the reaction time mentioned above, no further change in color was observed indicating that no more guest molecules were incorporated within the channels of the 3D-coordination polymers (host matrix). The products were isolated, washed several times with ethanol, and dried under vacuum.

Instruments

Elemental analysis was performed on a Perkin-Elmer 2400 automatic elemental analyzer. The X-ray diffractograms were measured on Debye–Scherrer PW 1050 (Cu_xK_α; Ni-Filter) instrument from Philips. IR spectra were recorded on Perkin-Elmer 683 spectrophotometer, applying KBr disk technique in the range of 4000–400 cm^{-1}. UV–VIS absorption spectra were recorded on a Shimadzu 3101 pc spectrophotometer as Nujol mull matrix. The thermogravimetric analyses (TGA) were performed on Shimadzu AT-50 thermal analyzer in the range 25 °C up to 800 °C with heating rate 10 °C/min in a nitrogen atmosphere. The electrical conductivity was measured by the two-prop technique on disks, obtained by pressing the samples at pressure of ca. 10 kg/cm^2 to form a cylindrical disk of diameter ca. 0.6 cm and thickness ca. 0.15 cm. The current, *I*, for the applied voltage, *V*, of the samples of high conductivity values was recorded using a Kiethly 175 A autoranging multimeter. Whereas, the resistance of the samples having low conductivity values was recorded using Kiethly 617 Programmable Electrometer.

Results and discussion

Analytical data

The stoichiometric ratios of the 3D-coordination polymers and supramolecular host–guest systems were calculated from the elemental analyses data (Table 1). Pyrrole and its derivatives react with the 3D-coordination polymers with an amount less or equal to 1 mol per 1 mol of the 3D-coordination polymers, except compound (3), in which pyrrole reacts with the 3D-coordination polymers III in the molar ratio 3:1, Table 1. This stoichiometric ratio was observed in the reaction of pyrrole with $[(Me_3E)_3Fe(CN)_6]_n$, E = Sn or Pb [14]. The results reveal that samples 2, 4–10, and 12 contain some water molecules. This result was confirmed by studying the TGA curves.

X-ray powder diffraction

Satisfactory agreement is found between the experimental powder X-ray diffractograms of I and II with the simulated diffractograms based on the data resulted from the structure analysis of single crystal X-ray studies of these compounds [6, 17], suggesting that the finely powdered bulk samples of I and II should be structurally closely related to the crystalline forms (Fig. 1). In the structure of I, every $Fe(CN)_6$ group is connected through Bu_3Sn bridges to six other $Fe(CN)_6$ units, forming three infinite nonlinear chains which interlinked into a 3D network. The $M(CN)_6$ units display a slightly distorted octahedral geometry and the Bu_3SnN_2 units are trigonal bipyramids with cyanide nitrogen atoms in the axial positions. These chains define various channels in the structure of I, which have a width of about 8.8 Å [6]. On the other hand, the structure of II reveals that a 3D structure with all six nitrogen atoms from the $Fe(CN)_6$ unit coordinated to tin atoms is not possible because of steric interference between the bulky Ph_3Sn groups. Thus, one of the CN groups bound to iron is not coordinated to a tin atom. Instead, its N atom is hydrogen bonded to the water molecule that is coordinated to a tin atom. There are three different types of infinite chains in the structure of II, which define stuffed channels down

Table 1 Composition, colors, and elemental analyses data of the 3D-coordination polymers and supramolecular host–guest systems

No.	Composition	Color	Elemental analysis		
			Found (calc.) %		
			C	H	N
I	$[(n\text{-}Bu_3Sn)_3Fe(CN)_6]_n$	Reddish brown	46.9 (46.6)	7.9 (7.5)	7.1 (7.8)
II	$[(Ph_3Sn)_3Fe(CN)_6]_n{\cdot}H_2O$	Brown	56.5 (56.3)	3.7 (3.7)	6.7 (6.6)
III	$[(n\text{-}Bu_3Sn)_2(Me_3Sn)Fe(CN)_6]_n$	Faint orange	41.8 (41.5)	6.8 (6.6)	8.6 (8.8)
IV	$[(n\text{-}Bu_3Sn)_2(Ph_3Sn)Fe(CN)_6]_n$	Reddish brown	50.7 (50.5)	6.7 (6.1)	7.4 (7.4)
V	$[(Ph_3Sn)_2(Me_3Sn)Fe(CN)_6]_n$	Brown	49.9 (50.2)	3.5 (3.6)	7.3 (7.8)
1	$[(Pyrrole)_1 + (I)]_n$	Black	48.4 (48.1)	7.0 (7.5)	8.2 (8.5)
2	$[(Pyrrole)_1 + (II)]_n{\cdot}5H_2O$	Black	53.7 (54.2)	3.9 (4.3)	7.1 (6.9)
3	$[(Pyrrole)_3 + (III)]_n$	Black	46.9 (46.7)	6.3 (6.8)	10.8 (10.9)
4	$[(Pyrrole)_1 + (IV)]_n{\cdot}3H_2O$	Black	48.9 (49.4)	5.7 (6.4)	8.2 (7.8)
5	$[(Pyrrole)_1 + (V)]_n{\cdot}3H_2O$	Black	48.4 (49.2)	4.1 (4.2)	8.9 (8.2)
6	$[(N\text{-}Methylpyrrole)_{0.8} + (I)]_n{\cdot}5H_2O$	Brown	44.2 (44.7)	8.1 (7.8)	7.5 (7.7)
7	$[(N\text{-}Methylpyrrole)_1 + (II)]_n{\cdot}10H_2O$	Faint green	51.0 (51.3)	4.9 (4.8)	5.6 (6.4)
8	$[(N\text{-}Methylpyrrole)_{0.8} + (III)]_n{\cdot}3H_2O$	Brown	41.3 (41.4)	6.2 (6.9)	8.0 (8.9)
9	$[(N\text{-}Methylpyrrole)_{0.8} + (IV)]_n{\cdot}5H_2O$	Buff	47.4 (48.1)	5.7 (6.6)	7.0 (7.3)
10	$[(N\text{-}Methylpyrrole)_{0.8} + (V)]_n{\cdot}10H_2O$	Gray	44.9 (44.6)	5.1 (4.9)	6.9 (7.2)
11	$[(2,5\text{-}Dimethylpyrrole)_{0.8} + (I)]_n$	Brown	48.8 (48.5)	7.0 (7.7)	8.9 (8.2)
12	$[(2,5\text{-}Dimethylpyrrole)_{0.8} + (II)]_n{\cdot}5H_2O$	Brown	54.7 (54.5)	5.0 (4.4)	6.2 (6.7)
13	$[(2,5\text{-}Dimethylpyrrole)_{0.9} + (IV)]_n$	Brown	52.0 (52.2)	5.8 (6.3)	7.2 (7.9)
14	$[(2,5\text{-}Dimethylpyrrole)_{0.9} + (V)]_n$n	Brown	52.1 (52.1)	4.0 (4.1)	8.4 (8.3)

different axes [17]. The comparison between the X-ray diffractograms of the novel mixed bridges 3D-coordination polymers (III–V) with that of their parents (Fig. 2) indicated that they are isostructural compounds, suggesting that the novel mixed bridges 3D-SCPs are a mixture of different connecting units, keeping the same polymeric nature [3, 6, 17]. The structures of these coordination polymers consist of trigonal-bipyramidal (tbp) $-C\equiv N-(R_3Sn)-N\equiv C-$ bridges acting as connecting units between the slightly distorted octahedral $Fe(CN)_6$ building blocks, forming three infinite nonlinear chains. The framework structures create wide parallel channels, which allow encapsulation of pyrrole derivatives. The increasing of steric bulk of the R group might force all C–N–Sn angles to become linear, resulting in a marked expansion of the lattice [2]. Changing the R group partially from methyl to butyl or phenyl should result in a higher point group symmetry for the iron atom that the connectivity of the 3D-lattice is changed, mostly simplified, because of the steric requirements of the butyl or phenyl groups.

The X-ray powder diffraction patterns of the supramolecular host–guest systems 1–14 (Fig. 3) indicate that they are isostructural compounds to the corresponding 3D-coordination polymers. This indicates that there is no change in the structure of the 3D-coordination polymers meanwhile the frameworks are little affected by the polymerization of pyrrole derivatives within their cavities. This phenomenon can be justified from the following IR spectra.

Infrared spectra

The IR spectra of the 3D-coordination polymers (I–V) reveal the presence of the vibrational bands corresponding to the $[Fe^{III}(CN)_6]^{3-}$ building blocks and the organotin groups (R_3Sn) or ($R_3'Sn$), (R and R′ = Me, *n*-Bu, or Ph) (Fig. 4; Table 2). The IR spectra exhibit only one intense band in the region 2140–2180 cm^{-1}, characteristic for the $\nu_{Fe^{III}-CN}$ frequencies of the $[Fe^{III}(CN)_6]^{3-}$ building blocks. In addition to, medium bands in the region 400–410 cm^{-1} due to asymmetric vibrations of the Fe^{III}–C bond. On the other hand, the medium bands observed within the range 515–598 cm^{-1} correspond to the various vibration modes of asymmetric vibrations of Sn–C bond. However, the absence of the symmetric vibrations of Sn–C bond advocates an exclusive presence of trigonal planar R_3Sn units which are axially anchoring to two cyanide N atoms [18]. In the case of 3D-coordination polymers (III–V), two types of the asymmetric ν_{Sn-C} are observed. This is due to the presence of two tbp configured R_3Sn and $R_3'Sn$ units. The presence of these bands indicates that these groups still play the role of linking the octahedral building blocks $[Fe^{III}(CN)_6]^{3-}$ through direct coordinate bond between the

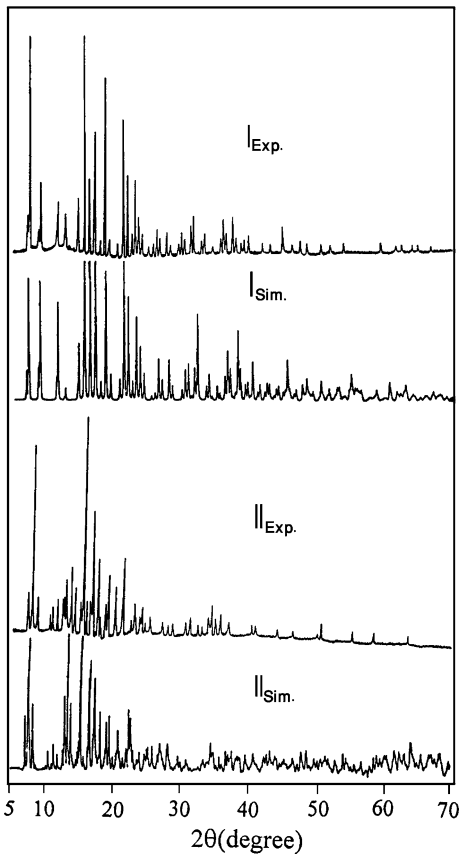

Fig. 1 Comparison of the X-ray powder diffraction with the simulated X-ray diffractogram of the single crystals of I and II

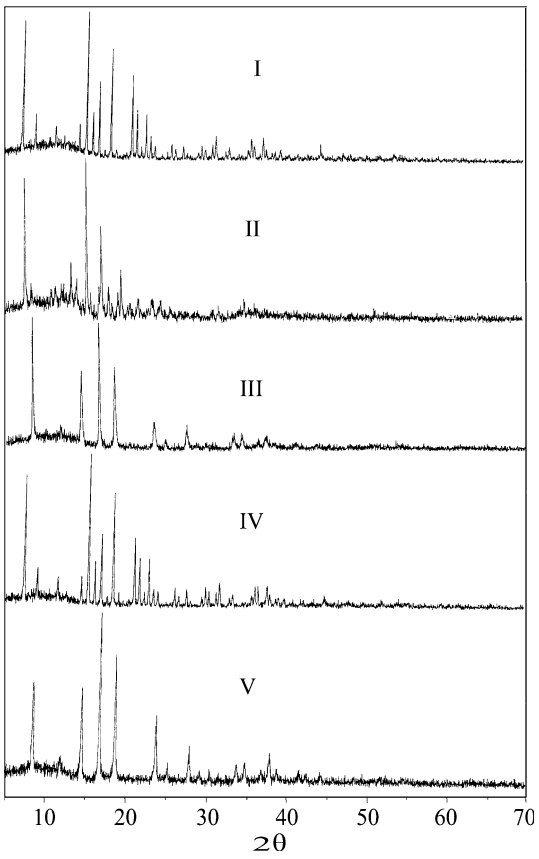

Fig. 2 X-ray diffractograms of the 3D-coordination polymers (III–V) and their parents I and II

nitrogen and the tin atoms. The IR spectra of the supramolecular host–guest systems 1–14 exhibit dramatic decrease in the relative intensity of the $\nu_{Fe^{III}-CN}$ band, while a new strong band appears in the region 2045–2089 cm^{-1} corresponding to the $\nu_{Fe^{II}-CN}$ (Fig. 4; Table 2). In addition, a new medium band appears in the region of 443–461 cm^{-1}corresponding to the $\nu_{Fe^{II}-C}$, indicating partial reduction of iron(III) to iron(II) by *N*-methylpyrrole and 2,5-dimethylpyrrole. In the case of the supramolecular host–guest systems 1–5 and 7, the corresponding 3D-coordination polymers are completely reduced to the isostructural anionic homologue $[(R_3Sn)_3Fe^{II}(CN)_6^-]_n$. This is gathered by the disappearance of the $\nu_{Fe^{III}-CN}$ and $\nu_{Fe^{III}-C}$ bands, while the medium band at 520 cm^{-1}, due to the stretching vibrations of Sn–C bond, does not show any significant changes, indicating that the tri-alkyl or aryl tin groups still play the role of linking the pairs of the iron-bonded cyanide ligands to form the 3D-network. Moreover, the IR spectra of the supramolecular host–guest systems 2, 4–10, and 12 show strong broad band in the region 3414–3505 cm^{-1} due to the ν_{OH} of the water molecules. On the other hand, the IR spectra of the supramolecular host–guest systems 1–14 (Fig. 4; Table 2) show the characteristic bands of the pyrrole compounds. The IR spectra of the

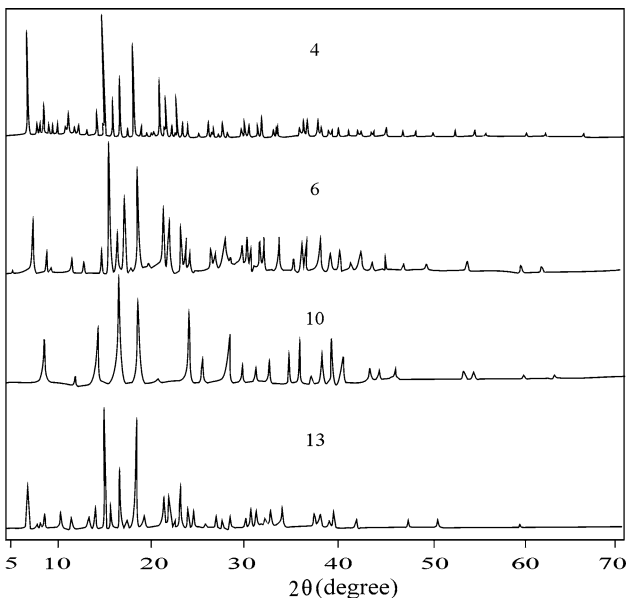

Fig. 3 X-ray powder diffraction of some of the host–guest systems

supramolecular host–guest systems 1–5 exhibit a medium band at ca. 1700 cm^{-1} corresponding to the stretching vibrations of the carbonyl group. This band becomes more

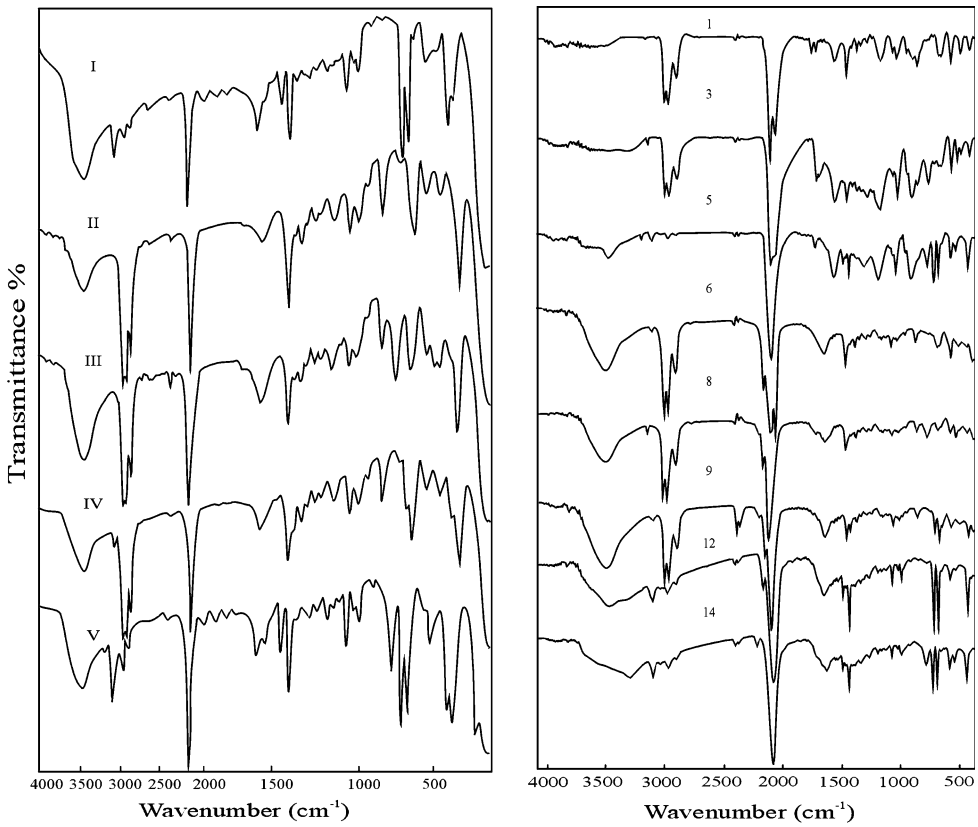

Fig. 4 Infrared spectra of the 3D-coordination polymers (I–V) and some of their host–guest systems

Table 2 IR spectral data (cm^{-1}) of the 3D-coordination polymers and supramolecular host–guest systems

No.	Guest						Host				
	ν_{OH}	ν_{NH}	ν_{CH}	$\nu_{C=O}$	$\nu_{C=C}$	ν_{C-N}	$\nu_{Fe^{III}-CN}$	$\nu_{Fe^{II}-CN}$	ν_{Sn-C}	$\nu_{Fe^{III}-C}$	$\nu_{Fe^{II}-C}$
I	–	–	–	–	–	–	2132	–	515	400	–
II	–	–	–	–	–	–	2141	–	582	408	–
III	–	–	–	–	–	–	2140	–	549	406	–
IV	–	–	–	–	–	–	2134	–	517, 598	402	–
V	–	–	–	–	–	–	2143	–	583, 551	410	–
1	–	3145	3032	1707	1560, 1460	1292	–	2089, 2045	520	–	443
2	2423	3136	3049	1705	1567, 1481	1302	–	2067	594	–	451
3	–	3198	3080	1710	1559, 1459	1291	–	2086, 2048	520	–	447
4	3505	3138	3050	1702	1567, 1459	1292	–	2085	524	–	451
5	3423	3154	3050	1705	1550, 1479	1303	–	2067	552	–	451
6	3428	–	3056	–	1564, 1460	1292	2136	2089, 2045	523	405	457
7	3445	–	3049	–	1578, 1481	1305	–	2076	548	–	452
8	3428	–	3080	–	1546, 1460	1291	2176, 2140	2086	552	418	461
9	3445	–	3054	–	1542, 1460	1293	2 182, 2134	2084	527	419	454
10	3428	–	3051	–	1521, 1480	1303	2 179	2074	553	–	452
11	–	3240	3080	–	1525, 1459	1291	2180	2086, 2045	545	418	453
12	3414	3239	3049	–	1515, 1480	1264	2138	2069	548	420	453
13	–	3248	3052	–	1518, 1459	1291	2176	2077	527	417	454
14		3245	3049		1524, 1480	1262	2189	2067	553	418	453

Scheme 1 Side reactions involved during the polymerization process

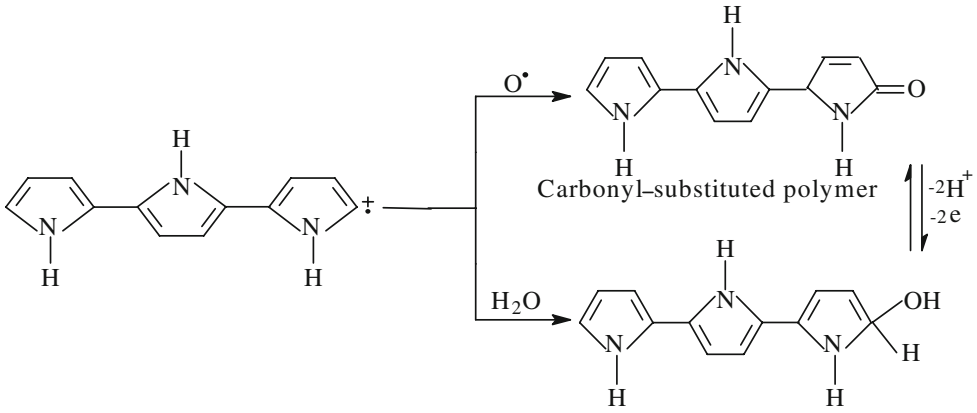

intense by the addition of few drops of water to the reaction mixture and disappears when the reaction is carried out under nitrogen atmosphere and strictly dry conditions [14]. The most acceptable suggestion about the origin of this band is the attack of the nucleophilic hydroxide ion to the radical cation of the polypyrrole unit during the polymerization process [19]. This observation reveals the occurrence of side reactions when atmospheric oxygen and water molecules are involved in the polymerization process and give rise to carbonyl-substituted polymers (Scheme 1).

Electronic absorption spectra

The spectra of the 3D-coordination polymers (I–V) reveal five intense bands around 220, 260, 300, 320, and 420 nm (Fig. 5; Table 3). These bands resemble the bands observed in the absorption spectrum of $K_3[Fe^{III}(CN)_6]$ at 219, 258, 300, 318, 333, and 419 nm [20]. The first band at 220 nm is due to π–π^* transitions from the metal to the cyanide ligand (M → L band). While, the three bands at 260, 300, and 420 nm have been identified as charge transfer transitions from the filled bonding orbitals, mainly of the cyanide ligand, to the hole in the shell of the central metal ion. They have been assigned as $^2T_{1u(\sigma)} \rightarrow {}^2T_{2g}$, $^2T_{2u(\pi)} \rightarrow {}^2T_{2g}$, and $^2T_{1u(\pi)} \rightarrow {}^2T_{2g}$, respectively [18]. The band of low intensity at 320 nm is due to ligand field (d–d) transitions of $[Fe^{III}(CN)_6]^{3-}$ building blocks. The other bands due to (d–d) transitions (ca. 285 and 370 nm) are obscured by the more intense broad bands due to L → M transitions [20, 21].

The electronic absorption spectra of the supramolecular host–guest systems 1–14 exhibit mainly five bands in the region 213–515 nm. These bands are due to the electronic transitions of pyrrole compounds and the 3D-coordination polymers. The first two bands appear at ca. 220 and 250 nm, due to the $^1L_a \leftarrow {}^1A$ and $^1L_b \leftarrow {}^1A$ transitions, respectively, of the pyrrole moieties within the channels of the 3D-coordination polymers. The electronic absorption spectra of the supramolecular host–guest systems 1–5 reveal band at ca. 372 nm. This band resembles the band of the in situ optical absorption spectra of polyaniline film on a conducting pt electrode [22]. This band does not observe in the spectra of the supramolecular host–guest systems 6–14 indicating that *N*-methylpyrrole and 2,5-dimethylpyrrole do not undergo polymerization within the channels of the 3D-coordination polymers. On the other hand, the spectra of the supramolecular host–guest systems 6 and 8–14 display broad bands in the regions 412–455 and 305–340 nm, due to π–π^* transitions of $[Fe^{III}(CN)_6]^{3-}$ and $[Fe^{II}(CN)_6]^{4-}$ building blocks, respectively. This indicates the presence of two iron environment within the channels of the supramolecular host–guest systems due to partial reduction of the hosts under the influence of guest molecules. In the case of the supramolecular host–guest systems 1–5 and 7, the 3D-coordination polymers are reduced to the isostructure Fe^{II}-homologue. This was confirmed by the presence of only one broad band in the region 306–340 nm due to the π–π^* transitions of $[Fe^{II}(CN)_6]^{4-}$ building blocks. The charge transfer character of these host–guest systems 1–14 was supported by the presence of new absorption bands in the region 448–515 nm corresponding to the intermolecular CT transitions between the 3D-coordination polymers and pyrrole guest compounds.

Thermogravimetric analysis

The thermograms of the 3D-coordination polymers I–V (Table 4) usually start by the decomposition of the easy volatile (R_3Sn) connecting units from the room temperature up to 270 °C, in addition to the gradual loss of cyanide groups as cyanogen molecules $(CN)_2$. Above ca. 270 °C, the cyanide-linked frame work is no longer stable and a structural breakdown occurs that finally involves oxidation of iron and tin to form oxides at ca. 420 °C. The thermolysis of III starts by the loss of one water molecule from the room temperature to 104 °C, confirming the elemental analyses data. On the other hand, the thermograms of the supramolecular host–guest

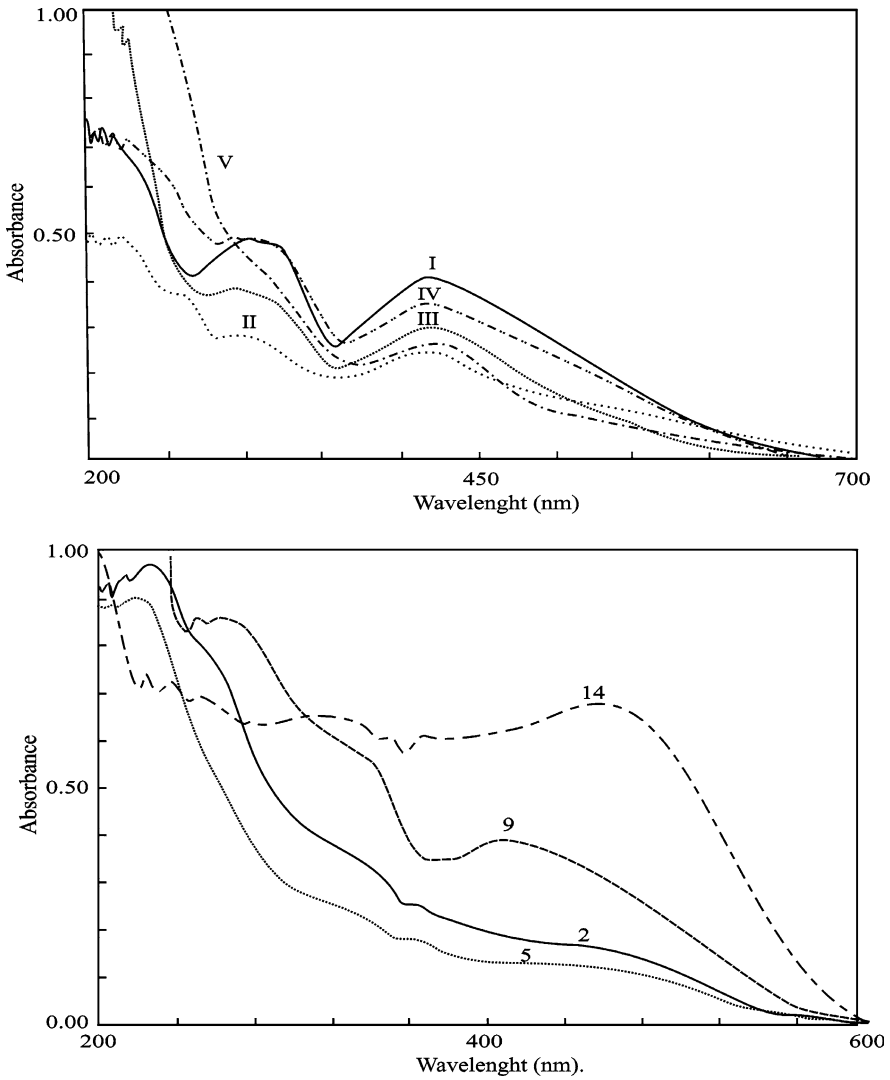

Fig. 5 The electronic absorption spectra (as Nujol mull) of the 3D-coordination polymers and some host–guest systems

systems 2, 4–10, and 12 exhibit multi-steps. During the first step, the water of crystallization is lost between the room temperature to 150 °C [23]. The coordinated water molecules and the guest moiety are released at the temperature range (150–390 °C) as well as the decomposition of the 3D-network, started by the decomposition of the (R_3Sn) connecting units in addition to the gradual loss of the cyanide groups. This step indicates that some of the water molecules are coordinated to some tin atoms O → Sn via the formation of the hydrogen bonding with cyanide group. At higher temperature up to 800 °C, the supramolecular host–guest systems suffer further complete decomposition to give a highly stable mixed oxide residue.

Magnetic measurements

All the 3D-coordination polymers I–V are paramagnetic with μ_{eff}, in the range of 2.08–2.50 BM. The paramagnetic behavior is due to the presence of low-spin iron(III), which has a $(dE)^5$electronic configuration with one unpaired electron in the d_{yz} orbital forming with the cyanide ions a distorted octahedral $[Fe^{III}(CN)_6]^{3-}$ structure [24, 25].

The host–guest SCPs 1–5 and 7 exhibit diamagnetic behavior. This result is due to complete reduction of $[Fe^{III}(CN)_6]^{3-}$ building blocks to $[Fe^{II}(CN)_6]^{4-}$ building blocks by pyrrole or *N*-methylpyrrole. On the other hand, the supramolecular host–guest systems 6 and 8–14 exhibit paramagnetic character in the range 1.03–1.22 BM due to the presence of stable octahedral $[Fe^{III}(CN)_6]^{3-}$ building blocks with large energy gap between the ground state $^2T_{2g}$ and the first excited state ^2E_g. The effective magnetic moment values of these supramolecular host–guest systems are less than the corresponding 3D-coordination polymers. This is attributed to the presence of mixed iron environment $[Fe^{III}(CN)_6]^{3-}$ and $[Fe^{II}(CN)_6]^{4-}$ building blocks indicating partial reduction of the 3D-SCPs by *N*-methylpyrrole and 2,5-dimethylpyrrole.

Table 3 The electronic absorption spectral data and the magnetic moments (BM) of the 3D-coordination polymers and supramolecular host–guest systems

No.	$^1L_a \leftarrow {}^1A$	$^1L_b \leftarrow {}^1A$	π–π^*			CT	μ_{eff} (BM)
			Polyemeraldine	Fe^{III}–CN	Fe^{II}–CN		
I	–	–	–	422	–	–	2.32
II	–	–	–	421	–	–	2.30
III	–	–	–	415	–	–	2.19
IV	–	–	–	417	–	–	2.23
V	–	–	–	422	–	–	2.46
1	220	245	371	–	330	450	–
2	225	260	370	–	338	480	–
3	218	240	375	–	320	448	–
4	218	250	371	–	330	465	–
5	225	262	373	–	325	480	–
6	217	238	–	418	305	493	1.02
7	228	259	–	–	340	507	–
8	219	251	–	412	306	453	1.22
9	216	241	–	412	310	478	1.07
10	218	260	–	450	335	505	1.03
11	215	245	–	440	327	500	1.15
12	220	263	–	451	323	500	1.10
13	215	258	–	455	331	511	1.01
14	213	248	–	402	320	515	1.19

Table 4 Thermogravimetric analyses data of some the 3D-coordination polymers and supramolecular host–guest systems

No.	Temperature ranges °C (weight loss %)				Final product calc. (found) %
	A	B	C	D	
I	27–246 (46.2)	246–800 (10.5)			$0.5Fe_2O_3 + 2.5SnO_2$ 43.6 (43.3)
II	30–104 (1.4)	104–248 (49.2)	248–800 (7.3)		$0.5Fe_2O_3 + 3SnO_2$ 41.6 (42.1)
III	22–175 (5.0)	175–246 (34.7)	246–800 (10.7)		$0.5Fe_2O_3 + 2.6SnO_2$ 49.3 (49.7)
IV	25–250 (40.3)	250–800 (12.6)			$0.5Fe_2O_3 + 3SnO_2$ 46.6 (47.1)
V	25–95 (4.2)	95–271 (33.1)	271–800 (12.9)		$0.5Fe_2O_3 + 3SnO_2$ 49.4 (49.2)
6	16–125 (2.1)	125–198 (9.7)	198–241 (28.0)	241–00 (15.6)	$0.5Fe_2O_3 + 3SnO_2$ 43.0 (44.6)
7	18–150 (5.5)	150–395 (41.8)	395–620 (9.8)	620–00 (7.8)	$0.5Fe_2O_3 + 3SnO_2$ 34.9 (35.1)
9	16–150 (6.8)	150–300 (39.9)	300–800 (11.3)		$0.5Fe_2O_3 + 3SnO_2$ 41.0 (42.0)
10	18–140 (6.2)	140–300 (36.8)	300–800 (16.2)		$0.5Fe_2O_3 + 3SnO_2$ 40.3 (40.8)
12	15–131 (6.4)	131–235 (37.0)	235–800 (23.3)		$0.5Fe_2O_3 + 2.6SnO_2$ 33.0 (33.3)

Conductivity measurements

All the 3D-coordination polymers I–V exhibit insulator character with conductivity values in the range of 10^{-10} -10^{-12} S cm^{-1}. This behavior is due to the absence of mobile electrons or ions. On the other hand, the supramolecular host–guest systems 1–5 behave as semiconductors having conductivities in the range 1.33×10^{-4} -2.88×10^{-6} S cm^{-1}. These values are less than that of the polypyrrole prepared by chemical polymerization or electropolymerization (in the range of 5×10^{-3}–10^{+2}), which is considered as a conducting polymers [26, 27]. It was found that the conductivity of polypyrrole is highly dependent on polymerization conditions as well as the steric interaction which affect the conjugation of the π-system and reduce the conductivity [28]. The low conductivity value may suggest that polypyrrole are present in the neutral form within the cavities of the 3D-coordination polymers [29]. The low conductivity reflects the absence of the metallic absorption around 1040 nm in the electronic absorption spectra of these supramolecular host–guest systems [28]. The semiconducting character of these compounds was supported by studying the variation of DC-electrical conductivity as a function of temperature (Fig. 6). The positive temperature coefficients of electrical conductivity indicating semiconducting behavior. By contrast, the host–guest SCPs 6-14 exhibit very low conductivity at room temperature in the range 2.86–7.35×10^{-12} S cm^{-1}. This is due to presence of the substituents at the pyrrole ring, where the conductivity decreases as the number of substituent increases [30].

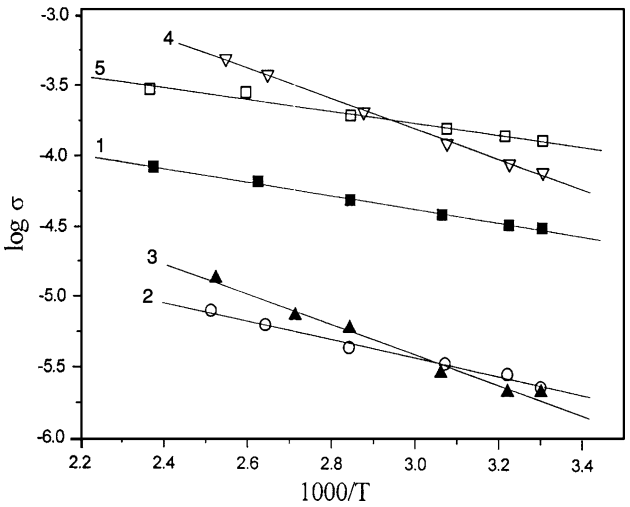

Fig. 6 Log σ_{rsus} 1000/T for the host–guest systems 1–5

Conclusion

It can be concluded that, pyrrole undergoes oxidative polymerization within the cavities of the 3D-SCPs to provide semiconducting supramolecular host–guest systems. The polymerization was assumed to proceed by a free radical mechanism involving formation of repeated dictation dimmers. The first step involves the oxidation of the monomer to radical cations. The next step is a coupling of two radical cations which mainly occurs in the α-position accompanied by deprotonation leading to a neutral dimer. Theoretical and experimental studies have indicated that the monomer subunits are incorporated into the chain preferentially through the α,α'-linkage due to the higher reactivity in α-position than in the β-position of the monomer [31–33]. Chain propagation then proceeds by oxidation of the neutral dimer to form the dimer radical cation, which can combine chemically with other monomeric, dimeric or oligomeric cation radicals to extend the chain (Scheme 2).

On the other hand, *N*-methylpyrrole and 2,5-dimethyl pyrrole are not polymerized, under these conditions, within the cavities of the 3D-coordination polymers. Generally, the presence of the substituents in α-position prevent electropolymerization process which occurs through

Scheme 2 Polymerization mechanism of pyrrole through radical–radical coupling

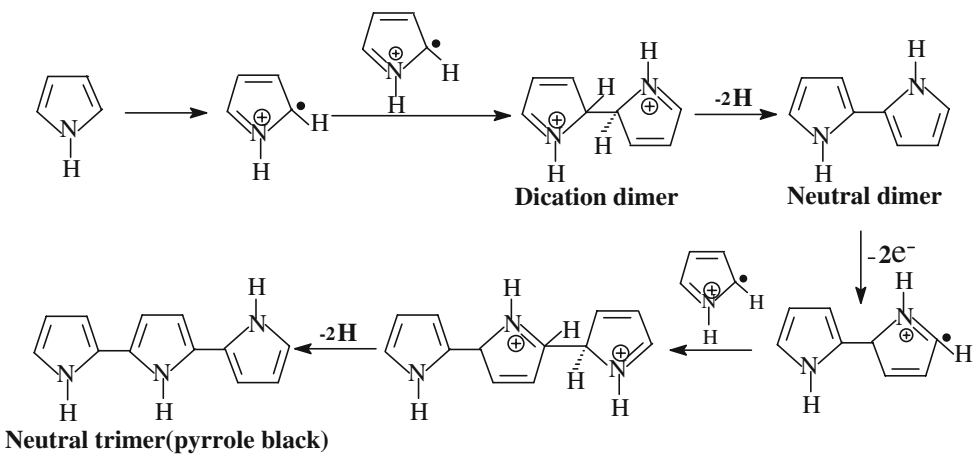

α,α′-linkage [33]. Therefore, the presence of two methyl groups in α,α′-positions, in the case of 2,5-dimethylpyrrole, prevent the chain propagation of the polymerization process. Also, *N*-methylpyrrole does not undergo polymerization within the cavities of the 3D-coordination polymers due to steric interaction which inhibit the polymerization process [34–36].

References

1. Steed JW, Atwood JL (2009) Supramolecular chemistry, 2nd edn. Wiley, New York
2. Yünlü K, Höck N, Fischer RD (1985) Angew Chem Int Ed Engl 24:879
3. Bonardi A, Carini C, Pelizzi C, Predieri G, Tarasconi P, Zoroddu MA, Molloy KC (1991) J Organometal Chem 401:283
4. Behrens U, Brimah AK, Soliman TM, Fischer RD, Apperley DC, Davies NA, Harris RK (1992) Organometallics 11:1718
5. Soliman TM, Etaiw SEH, Fendesak G, Fischer RD (1991) J Organomet Chem 415:C5
6. Niu T, Lu J, Wang X, Krop JD, Jacobson AJ (1998) Inorg Chem 37:5324
7. Niu T, Jacobson AJ (1999) Inorg Chem 38:5346
8. Eller S, Schwarz P, Brimah AK, Fischer RD (1993) Organometallics 12:3232
9. Ibrahim AMA, Etaiw SEH, Soliman TM (1992) J Organomet Chem 430:87
10. Hassanein M, Etaiw SEH (1993) Eur Polym J 29:47
11. Ibrahim MSh (2000) Transition Met Chem 25:695
12. Brandt P, Brimah AK, Fischer RD (1988) Angew Chem Int Ed Engl 27:1521
13. Etaiw SEH, Ibrahim AMA (1993) J Organomet Chem 456:229
14. Ibrahim AMA, Soliman TM, Etaiw SEH, Fischer RD (1994) J Organomet Chem 468:93 (and references therein)
15. Ibrahim MSh, Werida AH, Etaiw SEH (2003) Transition Met Chem 28:585
16. Ibrahim MSh, Werida AH, Etaiw SEH (2004) Phosphorus Sulfur Silicon 179:2441
17. Lu J, Harrison WTA, Jacobson AJ (1996) Inorgan Chem 35:4271
18. Ibrahim AMA (1999) Polyhedron 18:2711 (and references therein)
19. Osaka T, Momma M, Kanagwa H (1993) Chem Lett 22(4):649
20. Schmidtke HH, Evring G (1974) Z Physik Chem Neue Folge 925:211 (and references therein)
21. Gale R, McCaffery AJ (1973) J Chem Soc 13:1344
22. Monkman AP, Bloor D, Stevens GC, Stevens JCH (1987) J Phys D Appl Phys 20:1337
23. Rehbein M, Fischer RD, Epple M (2002) Thermochimica Acta 382:143
24. Nishida Y, Oshio S, Kida S (1977) Inorg Chim Acta 23:59
25. Beardwood P, Gibson FJ (1983) J Chem Soc Dalton Trans 4:737
26. Tourillon G, Garnier F (1982) J Electroanal Chem 135:173
27. Rapi S, Bocchi V, Gardini GP (1988) Synth Met 24:217
28. Salmon M, Diaz AF, Logan AJ, Krounbi M, Bargon J (1982) Mol Cryst Liq Cryst 83:265
29. Dong S, Ding J (1987) Synth Met 20:119
30. Etaiw SEH, Ibrahim AMA (1994) Thermochim Acta 233:297
31. Wei Y, Chan CC, Tian J, Jang GW, Hsueh KF (1991) Chem Mater 3:888
32. Kellogg RM (1984) In: Kartizky AR Rees CW (eds) Comprehensive heterocyclic chemistry, part 3, vol 4. Pergamon Press, Oxford, p 713
33. Diaz AF (1981) Chem Scr 17:145
34. Bidan G, Deronzier A, Moutet JC (1984) Nouv J Chim 8:501
35. Bidan G, Deronzier A, Moutet JC (1984) JCS Chem Commun 1185
36. Bidan G, Gugliemi M (1986) Synth Met 15:49